Chemical Engineering Journal 143 (2008) 308–313

Contents lists available at ScienceDirect

Chemical Engineering Journal

journal homepage: www.elsevier.com/locate/cej

An innovative method for effective micro-mixing of CO_2 gas during synthesis of nano-calcite crystal using sonochemical carbonization

S.H. Sonawane[a,*], S.R. Shirsath[b], P.K. Khanna[c], S. Pawar[a], C.M. Mahajan[a], V. Paithankar[a], V. Shinde[a], C.V. Kapadnis[a]

[a] Department of Chemical Engineering, Vishwakarma Institute of Technology, 666 Upper Indira Nagar, Bibwewadi, Pune, Maharashtra 411037, India
[b] Chemical Engineering Department, Sinhagad Institute of Technology, 44/1 Vadgaon (Budruk), Off Sinhgad Road, Pune, Maharashtra 400041, India
[c] Nanoscience Group Center for Materials for Electronics Technology (C-MET), Panchavati, Off Pashan Road, Pune C-MET 411008, India

ARTICLE INFO

Article history:
Received 9 March 2008
Received in revised form 19 May 2008
Accepted 21 May 2008

Keywords:
Nano-$CaCO_3$
Ultrasound
Carbonization
XRD

ABSTRACT

Synthesis of nano-$CaCO_3$ (nano-calcite) was carried out using sonochemical carbonization. CO_2 gas was used for carbonization of $Ca(OH)_2$. The effect of sonicator probe size (10, 14, and 20 mm diameter) on synthesis process was studied for constant ultrasonic power. Further, CO_2 gas was passed through sonicator probe drilled with hole along the length to investigate the effect on synthesis mechanism. The synthesis processes with and without ultrasound were compared. Similar comparison was done for synthesis, where ultrasonic probe used was with and without holes. The results showed that the application of ultrasound into the synthesis causes a super-saturation of Ca^{2+} ions in the synthesis leading to a rapid nucleation of $CaCO_3$ and improves the solute transfer rate. XRD gram shows that the nano-$CaCO_3$ obtained under sonication process gives the particle size of 35–50 nm, while without ultrasound it is 104 nm. Higher the probe size, there is a decrease in the particle size. The innovative arrangement of passing the gas through the probe instead of the separate sparger tube gives a reduction in the particle size. The preferred orientation of XRD peak for nano-$CaCO_3$ is observed to change from (1 0 1 0) plane to (1 1 9) plane in case of 20 and 14 mm probe diameter with hole.

1. Introduction

Inorganic nano-particle synthesis is a growing area of research. The change in the properties of materials with nanometric scale as compared with their bulk counterpart makes them increasingly suitable for variety of applications. Some of the properties of nanomaterials like large surface area, different crystal geometries, hydrophobicity make them more suitable for applications such as surface coatings, photocatalytic degradation, and catalytic activity and as flame retardant filler. Nano-inorganic particles such as $CaCO_3$, ZnO, TiO_2, and $Mg(OH)_2$ are being investigated for these applications since decades [1–5]. There are various methods available for nano-$CaCO_3$ synthesis such as batch carbonization [6], ultrasound-assisted synthesis [7], in situ deposition technique [8], micro-emulsion [9], etc. The method of synthesis affects the phase formation of nano-$CaCO_3$ crystals. Ultrasound synthesis has advantages over other methods in terms of narrow size particle size distribution. Nano-$CaCO_3$ has large commercial importance in terms of fillers in polymers and coatings, paper industry, etc. Nano-$CaCO_3$ may effectively improve the mechanical properties of the rubber because of the dramatic increase in the interfacial area between the nanoparticles and rubber [10–11]. It is used as coating layer on a base sheet of paper and can improve gloss, hiding power, etc [12]. Commercially synthesized nano-calcite uses conversion of calcite ore at higher temperature into CaO and then further hydrolyzed into $Ca(OH)_2$, and bubbling the CO_2 gas under controlled conditions. Control of nucleation and growth rate of crystal are key factors, which decide the narrow size distribution of the particles. Nucleation rate can be controlled using addition of surfactant or using ultrasonication. Number of authors studied nucleation and growth kinetics of nano-calcite during synthesis [13–17]. Reports show that Pandit and coworkers [18,19] have utilized the ultrasound power to incorporate the air into the reaction mass by breaking the interface of liquid and air for generation radicals. Lyczko et al. [20] studied the effect of ultrasound on primary nucleation of potassium sulphate by measuring the induction time and metastable zone width of unseeded solutions. They found that ultrasound allows induction time and metastable zone width to be significantly reduced in sonocrystallization process of potassium sulphate. Castro et al. [21] reported the positive effect of ultrasound

* Corresponding author Tel.: +91 20 24283001; fax: +91 20 24280926.
E-mail address: shirishsonawane@rediffmail.com (S.H. Sonawane).

1385-8947/$ – see front matter © 2008 Elsevier B.V. All rights reserved.
doi:10.1016/j.cej.2008.05.030

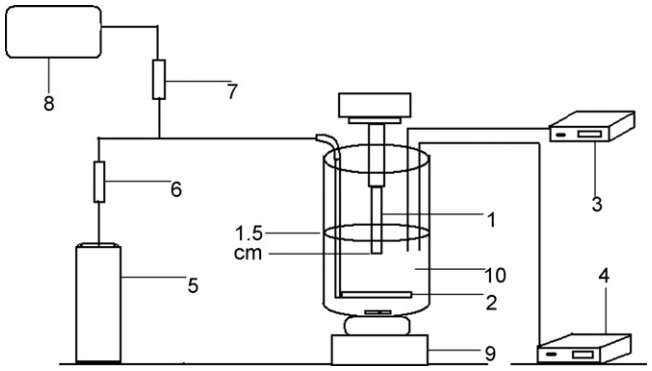

Fig. 1. Experimental set up for sonochemical carbonization experiments: 1, ultrasound probe; 2, CO_2 gas sparger; 3, conductivity meter; 4, pH meter; 5, CO_2 gas cylinder; 6, CO_2 gas flow meter; 7, air flow meter; 8, air compressor; 9, magnetic stirrer; 10, $Ca(OH)_2$ slurry.

on crystallization process is shown by dramatic reduction in the induction period, super-saturation and metastable zone. The results obtained showed that crystal size could be tailored by appropriate sonication conditions. Han et al. [22] studied the effect of flow rate and CO_2 content on the phase and morphology of $CaCO_3$ prepared by bubbling method. They found that more vaterlite is formed at a high flow rate or high CO_2 content, which attributes to the slowing down of the transformation of vaterlite to calcite. Vironea et al. [23] made first attempt to correlate the collapse pressure of the cavitating bubbles with the nucleation rate calculated from measured induction times for ammonium sulphate.

To achieve the effective utilization of CO_2 gas, which decides the efficiency of the process, we are proposing a new method of passing the reacting gas through the probe. Due to ultrasonic irradiation possible activation of the reaction could be attributed for generation of ions. In all these conditions, usually sparger is introduced into the system and CO_2 is sparged using a continuous supply for large-scale applications. The presence of sparger in a system can result in the decrease in the ultrasonic power transferred to the reactant due to scattering of sound waves. To avoid this, we suggest an innovative method for effective micro-mixing of CO_2 gas and utilization of ultrasonic power, during synthesis of nano-calcite crystals using sonochemical carbonization. We recommend small modification of ultrasonic probe as gas injector replacing sparger to avoid unnecessary power dissipation.

This manuscript investigates the effect of different ultrasound probes on carbonization reaction for nano-$CaCO_3$ synthesis. Effect of CO_2 gas passing through the probe was also investigated. This modification leads to different induction time due to which nucleation rate reduces, which can be confirmed from the crystallite size determined from XRD. The change in the preferred orientation of crystallites was observed in XRD; conclusion was drawn based on the observed results.

2. Experiment

2.1. Experimental set up

As shown in Fig. 1, batch-type sonochemical carbonization was carried out in 1 l reactor which consists of sonicator probe (Dakshin make, 240 W, 22 kHz) along with gas distribution plate, magnetic stirrer, CO_2 gas supply, N_2 and air supply. Small bubbles of 1 mm diameter were produced through the distributor plate. In other arrangement CO_2 gas was passed through the probe so as to get smaller size of gas bubbles which can easily take part in reaction and can help to increase the rate of reaction.

The ultrasound probe of 10, 14, and 20 mm diameter was used for ultrasound generation. Experiments were carried out with and without ultrasound and the results were compared. The reaction was monitored using conductivity and pH, whereas $Ca(OH)_2$ consumption was measured using conventional acid base titration. The synthesis was also carried out using all probes with hole (4 mm) drilled along length and diameter. The hole passage was used for effective micro-mixing of CO_2 gas.

2.2. Nano-$CaCO_3$ synthesis

The $Ca(OH)_2$ (analytical grade) was dissolved in HPLC grade water (millipore) to get the desired concentration. The suspension was completely mixed using magnetic stirrer at constant speed for 20 min. For all the experiments the diluted slurry of 4% mass fraction was prepared. Air and N_2 gas was also used to maintain the desired concentration of CO_2 gas and to flush the air from the reactor. CO_2 gas was passed into the carbonization unit consisting of diluted slurry to initiate the carbonization reaction. CO_2 gas flow rate was maintained at 50 LPH for all the experiments which was optimized for our system.

The total acoustic power injected into the sample was calculated using calorimetric method. Calorimetric method is generally used to determine the energy efficiency of the equipment [23]. In this methods, rise in temperature of fixed quantity of water in an insulated container over a given time was measured. Using this information, the actual power dissipated into a liquid can be calculated from the following equation:

$$\text{Power (W)} = m\,C_p\left(\frac{dT}{dt}\right) \quad (1)$$

where C_p is the heat capacity of the solvent ($J\,kg^{-1}\,K^{-1}$), m the mass of solvent (kg), dT the difference between the initial and final temperature (K) after a specific reaction time and dt is the time (s). Using this equation it was found the energy dissipated for the sonication was calculated W/m^3 for present system.

The conductivity, pH readings and burette readings were taken after fix time interval; each experiment was repeated twice in order to minimize the error in the readings.

2.3. Structural characterization

Structural properties of nano-$CaCO_3$ synthesized by the sonochemical carbonization process were analyzed using powder XRD grams of nano-$CaCO_3$ were recorded by means of X-ray diffractometer (Philips PW 1800). The Cu Kα radiation (LFF tube 35 kV, 50 mA) was selected for the analysis. Scanning electron microscopy (SEM) was done on Philips XL-30.

2.4. Particle size distribution

Particle size analysis was performed with NICOMP 380 (USA) submicron particle size analyzer. The measurement of particle size distribution of the nano-crystals was done by dynamic light scattering techniques (*via* a Laser input energy of 632 nm).

3. Result and discussion

Careful investigation of conductivity, pH and consumption rate of $Ca(OH)_2$ depicts lot of changes in ions especially Ca^{2+} and OH^- during the carbonization process. The reaction was stopped as soon as pH of the solution reached to 7, as there is no presence of $Ca(OH)_2$ resulting into the neutral solution. Fig. 2(a) describes the variation of conductivity with time for nano-calcite synthesized without ultrasound and using ultrasound probe with and without hole.

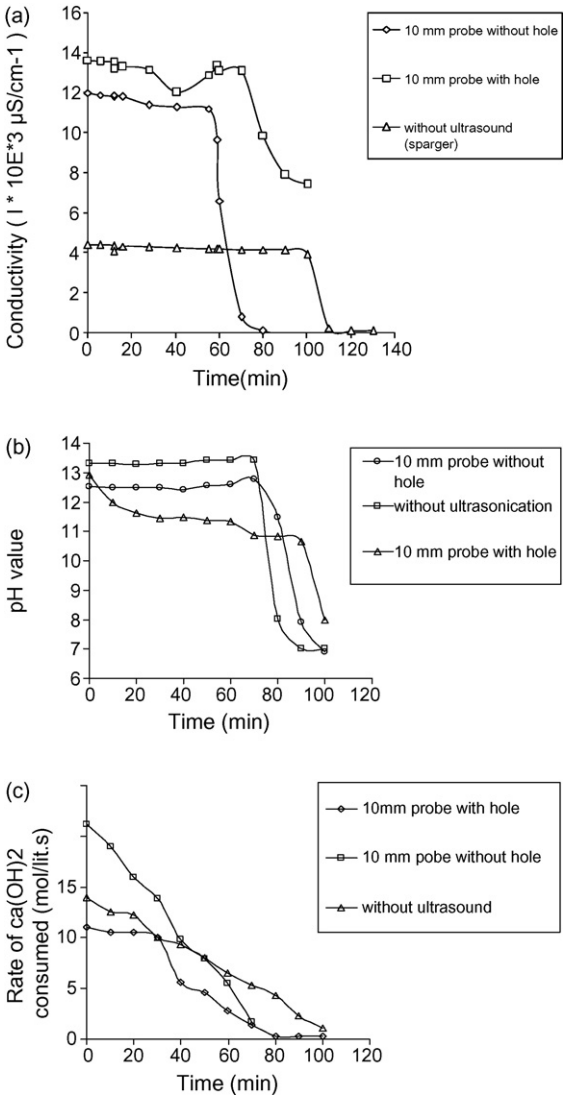

Fig. 2. Sample plots of changes in conductivity (a), pH value (b) and rate of $Ca(OH)_2$ consumed (c) in the solution vs. time in the presence of 10 mm probe sonication (passing the CO_2 through probe hole, without hole) and without ultrasound (using sparger).

Fig. 2(b) describes the variation of pH with time for nano-calcite synthesized without ultrasound and using ultrasound probe with and without hole. Fig. 2(c) describes the rate of consumption of $Ca(OH)_2$ during carbonization process for nano-calcite synthesized without ultrasound and using ultrasound probe with and without hole. Fig. 2(b) and (c) indicates that the pH is an independent parameter, which is not influenced by transfer of ions and is only dependent on the OH^- ion concentration. In the initial stage of reaction, pH of the reaction mass remains constant as there is no change in concentration of $Ca(OH)_2$ till the super-saturation occurs after which pH immediately decreases due to formation of nano-$CaCO_3$.

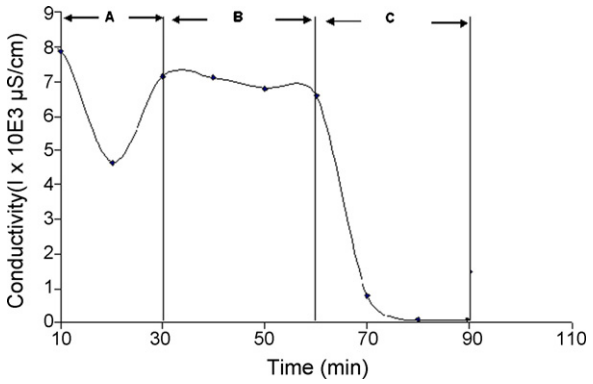

Fig. 3. Regions observed in the conductivity plots of 20 mm probe, passing the CO_2 gas through hole.

Fig. 3 shows conductivity readings of 20 mm probe with passing the CO_2 gas through hole. From Fig. 3 it is clear that conductivity readings are divided in the three regions. The first region gives information about the 'induction time', in which the nucleation of $Ca(OH)_2$ starts. It is also observed that in the first region 'A' there is one downward peak of conductivity with respect of time. The first downward peak indicates that massive nuclei of calcite are just formed attaching on to the surface of $Ca(OH)_2$ particles [24]. It is well known that lesser is the induction time, lesser is the crystal size. For the 20 mm probe, induction time is found reduced from 30 to 20 min, when CO_2 gas was passed through the probe. From Table 1, it is observed that the ultrasound has the significant effect onto the induction time and hence onto the particle size, further it is also possible to conclude that if the ultrasound probe is used with hole, there is a significant reduction in the induction time and this analysis was supported by observation of particles size obtained (Table 1). Power dissipation was also calculated using calorimetric method. Total power dissipated was found 18.5×10^3 W/m^3 for with hole experiment and 12.5×10^3 W/m^3 for without hole experiment. From Fig. 4a and b, it was found that the power dissipation plays important role in the reduction in the particle size. By increasing the probe size, there is an increase in the power dissipation for the liquid and hence inversely proportional to the particle size. It was also found that the probe with hole gives more dissipation of power into the reactor due to more surface area of the probe, hence higher power dissipation and reduction in particle size can be attributed for the probes with hole. It was also found that there is an exponential relationship between the ultrasound power injected and the particle size.

The XRD patterns (Fig. 5) show that the calcite powder synthesized by both with and without ultrasonication is crystalline in nature. The powder XRD is found preferably oriented along (0 1 0) plane for all samples, expect the case for ultrasonic probe (14 and

Table 1
Effect of ultrasound and without ultrasound on crystallite size, induction time and utilized energy during carbonization process

Probe diameter	Description	Total power dissipated into the reactor (W/m^3)	Crystallite size in nm	Particle size distribution (nm)	Induction time (min)
20	With hole	18.5×10^3	35	11–16	20
20	Without hole	12.5×10^3	51	24–29	30
14	With hole	11.6×10^3	38	26–37	32
14	Without hole	8.9×10^3	53	50–77	35
10	With hole	9.3×10^3	48	41–70	40
10	Without hole	5.0×10^3	60	69–106	60
No probe used	Reaction without ultrasound	–	104	62–117	110

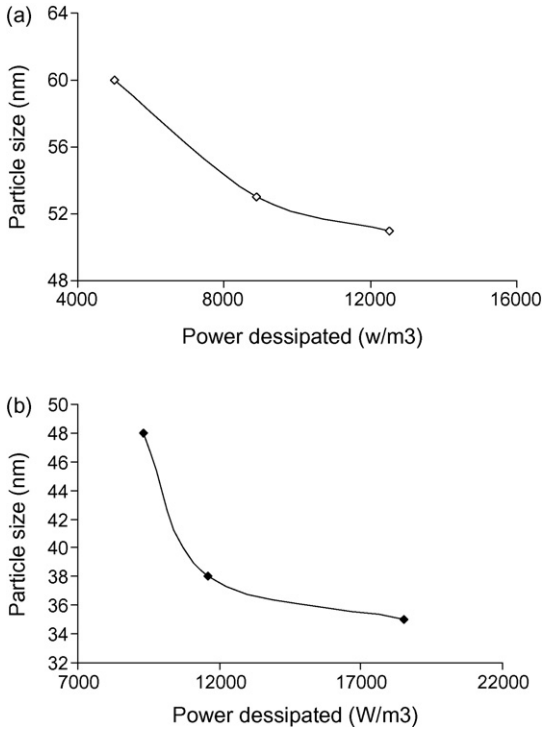

Fig. 4. (a) Effect of power dissipated onto the particle size of $CaCO_3$ crystal for probe without. (b) Effect of power dissipated onto the particle size of $CaCO_3$ crystal for probe with passing gas through hole.

20 mm diameter) with holes drilled along its diameter. The preferred orientation for latter was found to along (1 1 9) plane for both samples. The grain size was calculated of all the samples using Debye Scherrer's formula:

$$X_d = k\lambda/\beta\cos\theta \quad (2)$$

where k is the 0.9, β the FWHM and θ is the glancing angle of X-rays with the sample holder.

Cu Kα angel λ = 1.5405 Å radiation was used to obtain XRD patterns.

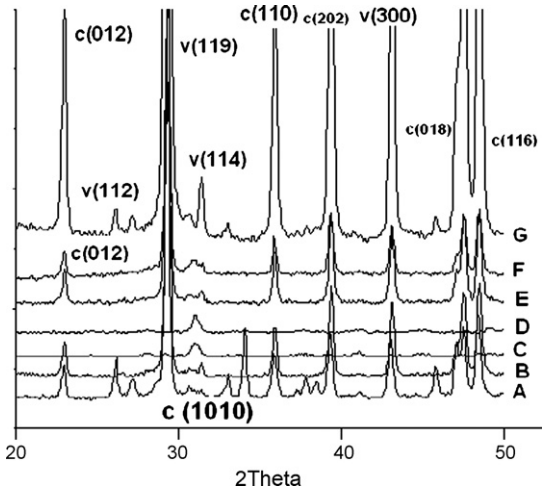

Fig. 5. XRD gram of nano-$CaCO_3$ crystals at different conditions (A) without ultrasound, (B) 10 mm probe without hole, (C) 10 mm probe with hole, (D) 14 mm probe without hole, (E) 14 mm probe with hole, (F) 20 mm probe without hole, and (G) 20 mm probe with hole.

The grain size of the calcite synthesized without ultrasonication was found to be 110 nm, whereas it was observed that the use of ultrasonication significantly reduces the grain size, consequently by increasing the surface area of the calcite synthesized and making it more suitable for the surface coatings applications such as improvement in the hiding power of coating along with TiO_2. Further, the effect of size of sonicator probe was also studied on structural properties of the nano-calcite. It was observed that the crystallite size is dependent on the diameter of the sonicator probe. The crystallite size was found to be decreased with an increase in diameter of sonicator probe as shown in Table 1. This must be because of increase in probe exposure area to the material when synthesis takes place.

In all experiments the CO_2 flow rate was maintained constant at 50 l/h. In order to study the effect of gas exposure area, the synthesis was also done by immersing the gas through the sparger as well as by drilling equidistant holes along the diameter of the probe and passing the gas through the probe so that it immerge out through the holes in the form of very fine and ultrasonically charged bubbles. This was done in order to increase the diffusion of gas into solution by activating the gas into ultrasonically charged fine bubbles. The effect on the structural properties was observed for both calcite synthesized by ultrasonic probe without hole and the probe with hole. The grain size was found to be dependent on CO_2 exposure area. The grain size decreased for all experiments where the gas was passed through the ultrasonic probe with holes as indicated in Table 1. The table clearly indicates the fact that ultrasonication increases the micro-mixing by further increasing the super-saturation which can be understood from significant decrease in the size of crystallites for all samples synthesized by ultrasonication when compared with the one without ultrasonication. It can be noted that further increase in probe diameter also causes decrease in grain size which may be because of the larger probe exposure area helps for improving micro-mixing. The grain size further found to be decreased with increasing the CO_2 exposure area (for 10, 14, and 20 mm probe with hole, the particle size found reduced from 48, 38, and 35 nm, respectively) It is evident that if CO_2 gas is passed through the ultrasonic probe with holes, the energized, fine gas bubbles formed in the reactant will give large surface area for the same volume of CO_2 gas. The particle size decreases for the probe with hole can be attributed to the fact that the consumption rate of the CO_2 gas by unit mass of calcium hydroxide becomes higher than the gas absorption rate, in case where the probe used is without hole and the gas is passed directly in reactant solution using sparger tube. In this case the absorption of CO_2 gas controls the grain size of the product. It can be noted that similar kinds of results obtained by Mingzahao et al. [7] for different CO_2 flow rates. Mingzahao et al. report that with increase in the CO_2 flow rate grain size decreases significantly. However, it is important to note that without changing the flow rate similar effects could be obtained only by increasing the gas exposure area with the help of the ultrasonic probe carrying CO_2 gas through holes. This clearly indicates the fact that the rate of reaction increases with increase in the gas exposure area. Further the preferred orientation of $CaCO_3$ powder was found to be changed from (1 0 1 0) plane to (1 1 9) plane for samples synthesized by ultrasonic probe (14 mm and 20 mm diameter) without holes when XRD patterns were compared with those synthesized by same probes with holes drilled along the diameter [25]. The above observation indicates that the increase in gas exposure area due to ultrasonically charged bubbles plays the important role in growth mechanism of $CaCO_3$ powder. This may be responsible for the change in preferred orientation of the synthesized powder. Fig. 6 shows the SEM morphology of nano-$CaCO_3$ particles prepared under the 20 mm probe and passing the CO_2 gas through hole, the SEM image shows that the nano-$CaCO_3$ particles are found to be perfect spherical in shape.

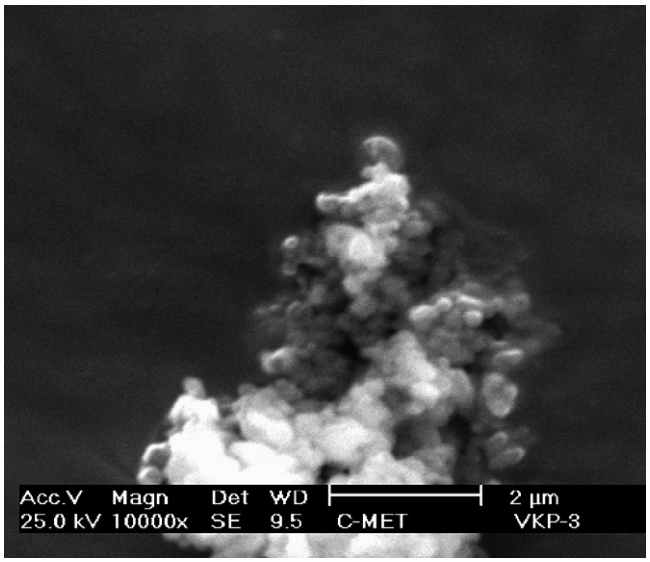

Fig. 6. SEM image of nano-$CaCO_3$ particles of 20 mm probe with hole.

The particle size distribution of the powders prepared by using the 20 mm probe with hole and without hole is given in Fig. 7. It is observed that the 20 mm probe with hole gives narrow size distribution in the range of 11–16 nm, with average particle size of 13 nm (Fig. 7A). While the powder obtained by using the 20 mm probe without hole gives the particle size distribution in the range of 24–30 nm with average particle size of 27 nm (Fig. 7B). It is also observed that the reaction carried out without ultrasound gives the wide range of particle size distribution with 62–117 nm (Fig. 7C).

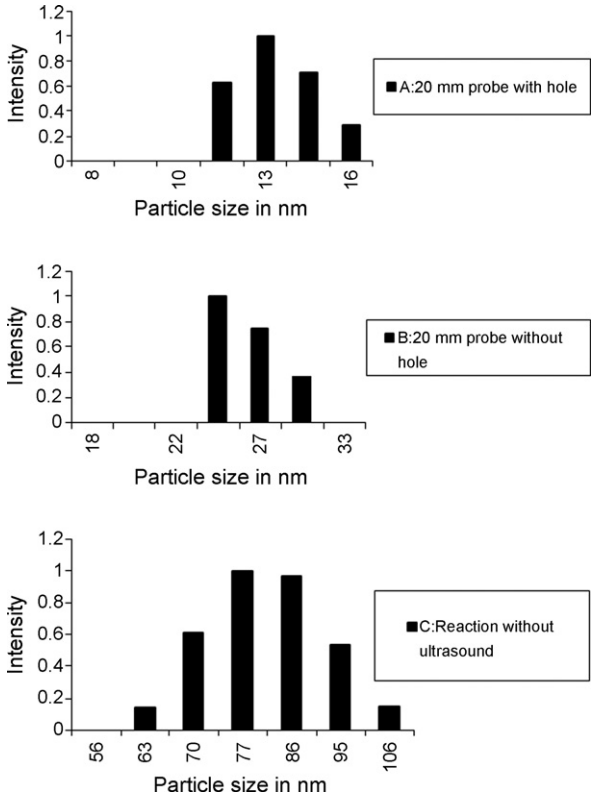

Fig. 7. Particle size distribution of nano-$CaCO_3$ particles for (A) 20 mm probe with hole, (B) 20 mm probe without hole and (C) reaction without ultrasound.

4. Conclusion

Passing the gas through the probe hole gives significant improvement in the reduction of particle size. Micro-mixing of the CO_2 gas through the probe leads to change in the preferred orientation of nano-calcite crystals. There is also significant effect of ultrasound power dissipated in the reactor; the power dissipated and the particle size on exponential relationship. The conductivity variation with time shows that the induction time is reduced and has advantages for the specific industrial applications such as hiding power improvement in the surface coatings.

Acknowledgments

S.H. Sonawane acknowledges the Department of Science and Technology (Govt. of India) for providing the funding under the grant number SR/FTP/ETA-35/2007. Authors are also thankful to Prof. Dr A.B. Pandit (UICT, Mumbai) for his valuable suggestion to carry out the experimental work.

References

[1] S. Mishra, S.H. Sonawane, A. Bendale, K. Patil, Mechanical and flame retarding properties of PP filled with nano-$Mg(OH)_2$, J. Appl. Polym. Sci. 94 (2004) 116–122.
[2] J. Wang, Y. Jiang, Z. Zhang, G. Zhao, G. Zhang, T. Ma, W. Sun, Investigation on the sonocatalytic degradation of Congo red catalyzed by nanometer rutile TiO_2 powder and various influencing factors, Desalination 216 (2007) 196–208.
[3] J. Németh, G. Rodríguez-Gattorno, D. Díaz, R. América, V. Olmos, I. Dékány, Synthesis of ZnO nanoparticles on a clay mineral surface in dimethyl sulfoxide medium, Langmuir 20 (2004) 2855–2860.
[4] S.H. Sonawane, V. Chitodkar, S. Mishra, Characterization and mechanical properties of epoxy-$CaCO_3$ nano-composites, Polym. Plast. Technol. Eng. 44 (2005) 463–473.
[5] C.M. Chan, J. Wu, J.X. Li, Y.K. Cheung, Polypropylene/calcium carbonate nanocomposites, Polymer 43 (2002) 2981–2992.
[6] V.A. Juvekar, M.M. Sharma, Absorption of CO_2 in suspension of lime, Chem. Eng. Sci. 28 (1973) 825–837.
[7] H. Mingzhao, E. Forssberg, Y. Wang, Y. Han, Ultrasonication-assisted synthesis of calcium carbonate nanoparticles, Chem. Eng. Commun. 192 (11) (2005) 1468–1481.
[8] S. Mishra, S.H. Sonawane, Studies on characterization of nano-$CaCO_3$ prepared by in situ deposition technique and its application in PP nano-composites, J. Polym. Sci. B: Polym. Phys. 43 (2005) 107–113.
[9] M.V. Degaonkar, A. Mehra, R. Jain, H.J. Heeres, Synthesis of $CaCO_3$ nanoparticles by carbonation of lime solutions in reverse micellar systems, Chem. Eng. Res. Des. 82 (A11) (2004) 1438–1443.
[10] H.H. Cai, S.D. Li, G.R. Tian, Reinforcement of natural rubber latex film by ultrafine calcium carbonate, J. Appl. Polym. Sci. 87 (2003) 982–985.
[11] M. Avella, M.L. Dilorenzo, M.E. Errico, E. Martuscelli, Novel PMMA/$CaCO_3$ nanocomposites abrasion resistant prepared by an in situ polymerization process, Nano Lett. 1 (2001) 213–217.
[12] R.D. Kulkarni, S.H. Sonawane, S. Mishra, Utilization of nano-extenders for part replacement of TiO_2 for enhancement of hiding power of surface coatings, Indian Patent 11/mum/2004.
[13] R.Y. Lin, J.Y. Zhang, Y.G. Bai, Mass transfer of reactive crystallization in synthesis calcite nanocrystal, Chem. Eng. Sci. 61 (2006) 7019–7028.
[14] Z. Guo, A.G. Jones, N. Li, The effect of ultrasound on the homogeneous nucleation of $BaSO_4$ during reactive crystallization, Chem. Eng. Sci. 61 (2006) 1617–1626.
[15] R.Y. Lin, J.Y. Zhang, P.X. Zhang, Nucleation and growth kinetics in synthesizing nanometer calcite, J. Cryst. Growth 245 (2002) 309–320.
[16] K. Sawada, The mechanisms of crystallization and transformation of calcium carbonates, Pure Appl. Chem. 69 (5) (1997) 921–928.
[17] C.Y. Tai, P.C. Chen, S.M. Shih, Size-development growth and contact nucleation of calcite crystals, AIChE 39 (1993) 1472–1482.
[18] A. Kumar, P. Gogate, A.B. Pandit, A.M. Wilhelm, H. Delmas, Investigation of induction of air due to ultrasound source in the sonochemical reactors, Ultrason. Sonochem. 12 (2005) 453–460.
[19] P.R. Gogate, R.K. Tayal, A.B. Pandit, Cavitation: a technology on the horizon, Curr. Sci. 91 (2006) 1–12.
[20] N. Lyczko, F. Espitalier, O. Louisnard, J. Schwartzentruber, Effect of ultrasound on the induction time and the metastable zone widths of potassium sulphate, Chem. Eng. J. 86 (2002) 233–241.
[21] M.D. Luque De Castro, F. Priego, Capote ultrasound assisted crystallization (sonocrystallization), Ultrason. Sonochem. 14 (2007) 717–724.

[22] Y.S. Han, G. Hadiko, M. Fuji, M. Takahashi, J. Cryst. Growth 276 (2005) 541–548.
[23] C. Vironea, H.J.M. Kramera, G.M. van Rosmalena, A.H. Stoopb, T.W. Bakkerb, Primary nucleation induced by ultrasonic cavitation, J. Cryst. Growth 294 (2006) 9–15.
[24] S. Zhang, Y. Han, J. Jiang, H. Wang, Studies of crystallization of nano-calcium carbonate in the reaction system $Ca(OH)_2$-H_2O-CO_2, J. Northeastern Univ. Nat. Sci. 21 (2000) 169–172.
[25] JCPDS data sheet for $CaCO_3$, 24–27, set 23–24.